QUANTUM LONG SHORT-TERM MEMORY

[1]*Samuel Yen-Chi Chen,* [1]*Shinjae Yoo,* [1]*Yao-Lung L. Fang*

[1]Computational Science Initiative, Brookhaven National Laboratory, Upton, NY 11973, USA

ABSTRACT

Long short-term memory (LSTM) is a kind of recurrent neural networks (RNN) for sequence and temporal dependency data modeling and its effectiveness has been extensively established. In this work, we propose a hybrid quantum-classical model of LSTM, which we dub QLSTM. We demonstrate that the proposed model successfully learns several kinds of temporal data. In particular, we show that for certain testing cases, this quantum version of LSTM converges faster, or equivalently, reaches a better accuracy, than its classical counterpart. Due to the variational nature of our approach, the requirements on qubit counts and circuit depth are eased, and our work thus paves the way toward implementing machine learning algorithms for sequence modeling such as natural language processing, speech recognition on noisy intermediate-scale quantum (NISQ) devices.

Index Terms— Quantum machine learning, Variational quantum circuits, Long short-term memory and Recurrent neural network

1. INTRODUCTION

Recently, machine learning (ML), in particular deep learning (DL), has found tremendous success in computer vision [1, 2, 3], natural language processing [4], and mastering the game of Go [5]. One of the most commonly used ML architectures is *recurrent neural networks* (RNN), which is capable of modeling sequential data. RNNs have been applied to study several natural language processing tasks such as machine translation [4], speech recognition [6] as well as other signal processing and function approximation tasks in scientific research [7, 8].

In the meantime, quantum computers, both general- and special-purpose ones, are introduced to the general public by several technology companies such as IBM [9], Google [10], and D-Wave [11]. While in theory quantum computers can provide exponential speedup to certain classes of problems and simulations of highly-entangled physical systems that are intractable on classical computers, quantum circuits with a large number of qubits and/or a long circuit depth cannot yet be faithfully executed on these noisy intermediate-scale quantum (NISQ) devices [12] due to the lack of quantum error correction [13, 14]. Therefore, it is non-trivial to design an application framework that can be potentially executed on the NISQ devices with meaningful outcomes.

Recently, Mitarai *et al.* proposed variational quantum algorithms, circuits, and encoding schemes [15] which are potentially applicable to NISQ devices. These quantum algorithms successfully tackled several simple ML tasks, including function approximation and classification. It takes advantage of quantum entanglement [15, 16] to reduce the number of parameters in a quantum circuit, and iterative optimization procedures are utilized to update the circuit parameters. With such an iterative process, the noise in quantum devices can be effectively absorbed into the learned parameters without incorporating any knowledge of the noise properties. With these in hand, hybrid quantum-classical algorithms becomes viable and could be realized on the available NISQ devices. Such variational quantum algorithms have succeeded in classification tasks [17, 18], generative adversarial learning [19] and deep reinforcement learning [20]. However, the problem of learning sequential data, to our best knowledge, has not been investigated thoroughly in the quantum domain.

In this work, we address the issue of learning sequential, or temporal, data with quantum machine learning (QML) [21, 22, 23]. We propose a novel framework to demonstrate the feasibility of implementing RNNs with *variational quantum circuits* (VQC) — a kind of quantum circuits with gate parameters optimized (or trained) classically — and show that quantum advantages can be harvested in this scheme. Specifically, we implement long short-term memory (LSTM) — a famous variant of RNNs capable of modeling long temporal dependencies — with VQCs, and we refer to our QML architecture as *quantum* LSTM, or QLSTM for brevity. In the proposed framework, we use a hybrid quantum-classical approach, which is suitable for NISQ devices through iterative optimization while utilizing the greater expressive power granted by quantum entanglement. Through numerical simulations we show that the QLSTM learns faster (takes less epochs) than the classical LSTM does with a similar number of network parameters. In addition, the convergence of our QLSTM is more stable than its classical counterpart; specifically, no peculiar spikes that are typical in LSTM's loss functions is observed with QLSTM.

This paper is organized as follows. First, in Section 2 we introduce VQCs, the building block of the proposed framework. Next, we discuss our QLSTM architecture and its detailed mechanism in Section 3. In Section 4 we investigate through simulations the QLSTM capability for several different kinds of temporal data and compare with the outcomes of their classical counterparts. Finally, we conclude in Section 5.

2. VARIATIONAL QUANTUM CIRCUITS

VQCs are a kind of quantum circuits that have *tunable* parameters subject to iterative optimizations, see Figure 1 for a generic VQC architecture. There, the $U(\mathbf{x})$ block is for the state preparation that encodes the classical data $\mathbf{x}$ into the quantum state of the circuit and is not subject to optimization, and the $V(\boldsymbol{\theta})$ block represents the variational part with *learnable* parameters $\boldsymbol{\theta}$ that will be optimized through gradient methods. Finally, we measure a subset (or all) of the qubits to retrieve a (classical) bit string like 0100.

Previous results have shown that such circuits are robust against quantum noise [24, 25, 26] and therefore suitable for the NISQ devices. VQCs have been successfully applied to function approximation [15], classification [17, 18, 27, 28], generative modeling [19], deep reinforcement learning [20], and transfer learning [29]. Furthermore, it has been pointed out that the VQCs are more expressive

Fig. 1: Generic architecture for variational quantum circuits (VQC). $U(\mathbf{x})$ is the quantum routine for encoding the (classical) input data $\mathbf{x}$ and $V(\boldsymbol{\theta})$ is the variational circuit block with tunable parameters $\boldsymbol{\theta}$. A quantum measurement over some or all of the qubits follows.

than classical neural networks [30, 11, 16] and so are potentially better than the latter. Here, the *expressive power* refers to the ability to represent certain functions or distributions with a limited number of parameters. Indeed, artificial neural networks (ANN) are said to be *universal approximators* [31], meaning that a neural network, even with only one single hidden layer, can in theory approximate any computable function. As we will see below, using VQCs as the building blocks of quantum LSTM enables faster learning.

3. QUANTUM LSTM

In this paper, we extend the classical LSTM into the quantum realm by replacing the classical neural networks in the LSTM cells with VQCs, which would play the roles of both feature extraction and data compression, see Figure 3 for a schematic of the proposed QLSTM architecture. The VQC components used in QLSTM are shown in Figure 2. The VQC is composed of three major parts: *data encoding*, *variational layer* and *quantum measurements*. The data encoding circuit is used to transform the classical vector (input) into a quantum state. The variational layer is the actual learnable components, with circuit parameters updated via gradient descent algorithms. Finally, the quantum measurements are used to retrieve the values for further processing. On a real quantum computer, multiple circuit runs can be carried out for the expectation values. In this work, we use simulation software to calculate the expectation values analytically. The mathematical construction of QLSTM is given in Equation 1.

Fig. 2: Generic VQC architecture for QLSTM. It consists of three layers: the data encoding layer (with the H, R_y, and R_z gates), the variational layer (dashed box), and the quantum measurement layer. Note that the number of qubits and the number of measurements can be adjusted to fit the problem of interest, and the variational layer can contain several dashed boxes to increase the number of parameters, all subject to the capacity and capability of the quantum machines used for the experiments.

$$f_t = \sigma\left(VQC_1(v_t)\right) \tag{1a}$$

$$i_t = \sigma\left(VQC_2(v_t)\right) \tag{1b}$$

$$\tilde{C}_t = \tanh\left(VQC_3(v_t)\right) \tag{1c}$$

$$c_t = f_t * c_{t-1} + i_t * \tilde{C}_t \tag{1d}$$

$$o_t = \sigma\left(VQC_4(v_t)\right) \tag{1e}$$

$$h_t = VQC_5(o_t * \tanh\left(c_t\right)) \tag{1f}$$

$$y_t = VQC_6(o_t * \tanh\left(c_t\right)), \tag{1g}$$

Fig. 3: The proposed quantum long short-term memory (QLSTM) architecture. Each *VQC* box is of the form as detailed in Figure 2. The σ and $\tanh$ blocks represent the sigmoid and the hyperbolic tangent activation function, respectively. x_t is the input at time t, h_t is for the hidden state, c_t is for the cell state, and y_t is the output. $\otimes$ and $\oplus$ represents element-wise multiplication and addition, respectively.

4. EXPERIMENTS AND RESULTS

In this section we study and compare the capability and performance of the QLSTM with its classical counterpart. Specifically, we study QLSTM's capability to learn the representation of various functions of time. We present numerical simulations of the proposed QLSTM architecture applied to several scenarios.

To make a fair comparison, we employ a classical LSTM with the number of parameters comparable to that of the QLSTM. The classical LSTM architecture is implemented using PyTorch [32] with the hidden size 5. It has a linear layer to convert the output to a single target value y_t. The total number of parameters is 166 in the classical LSTM. As for the QLSTM, there are 6 VQCs (Figure 3), in each of which we use 4 qubits with depth $= 2$ in the variational layer. In addition, there are 2 parameters for the final scaling. Therefore, the number of parameters in our QLSTM is $6 \times 4 \times 2 \times 3 + 2 = 146$. We use the same (Q)LSTM architecture throughout this section. Finally, we use PennyLane [33, 34] and Qulacs [35] for the simulation of quantum circuits, and train the QLSTM in the same PyTorch framework applied to LSTM.

We consider the following scheme for training and testing: the (Q)LSTM is expected to predict the $(N + 1)$-th value given the first N values in the time sequence. For example, at step t if the input is $[x_{t-4}, x_{t-3}, x_{t-2}, x_{t-1}]$ (i.e., $N = 4$), then the QLSTM is expected to generate the output y_t, which should be close to the ground truth x_t. We set $N = 4$ throughout. For data generated by mathematical functions, we rescale them to the interval $[-1, 1]$. We use the first

67% elements in the sequence for training and the rest (33%) for testing. For each experiment, we train with maximum 100 epochs.

The optimization method is chosen to be RMSprop [36], a variant of gradient descent methods with an adaptive learning rate that updates the parameters θ as:

$$E\left[g^2\right]_t = \alpha E\left[g^2\right]_{t-1} + (1-\alpha)g_t^2, \tag{2a}$$

$$\theta_{t+1} = \theta_t - \frac{\eta}{\sqrt{E\left[g^2\right]_t} + \epsilon}g_t, \tag{2b}$$

where g_t is the gradient at step t and $E\left[g^2\right]_t$ is the weighted moving average of the squared gradient with $E[g^2]_{t=0} = g_0^2$. The hyperparameters are set as follows for both LSTM and QLSTM: learning rate $\eta = 0.01$, smoothing constant $\alpha = 0.99$, and $\epsilon = 10^{-8}$.

4.1. Periodic Functions

We first investigate our QLSTM's capability in learning the sequential dependency in periodic functions. Without loss of generality we consider the sine function, a simple periodic function with constant amplitude and period:

$$y = \sin(x) \tag{3}$$

It is expected that such a function is easier to model or represent compared to functions with time-dependent amplitudes or more structure, which we discuss later. The result is shown in Figure 4. By comparing the results from different epochs, it can be seen that both the QLSTM and LSTM successfully learn the sine function. While both of them converge well, we point out that the QLSTM learns significantly more information after the first training epoch than the LSTM does. For example, QLSTM's training loss at Epoch 15 is slightly lower than LSTM's (see Table 1), a trend that will become more evident later). In addition, QLSTM's loss is more stably decreasing than LSTM's; there are no spikes in the quantum case (see the right panels in Figure 4).
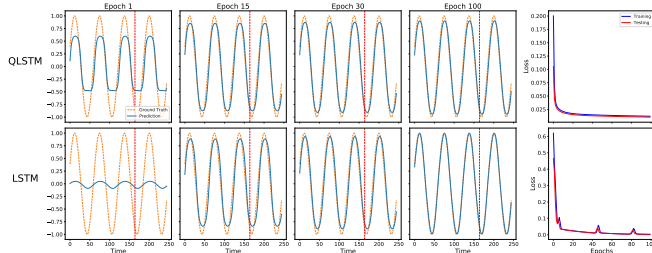
Fig. 4: Learning the sine function. QLSTM already learns the essence of $\sin(x)$ by Epoch 1, and has no peculiar bumps in the loss function. The orange dashed line represents the ground truth $\sin(x)$ [that we train the (Q)LSTM to learn] while the blue solid line is the output from the (Q)LSTM. The vertical red dashed line separates the *training* set (left) from the *testing* set (right).

	Training Loss	Testing Loss
QLSTM	1.89×10^{-2}	1.69×10^{-2}
LSTM	2.86×10^{-2}	2.81×10^{-2}

Table 1: The comparison of loss values at Epoch 15 for the sine function experiment.

4.2. Physical Dynamics

In this part of the experiments, we study the capability of the proposed QLSTM in learning the sequential dependency in physical dynamics.

4.2.1. Damped harmonic oscillator

Damped harmonic oscillators are one of the most classic textbook examples in science and engineering. It can describe or approximate a wide range of systems, from mass on a spring to electrical circuits. The differential equation describing the damped simple harmonic oscillation is,

$$\frac{d^2x}{dt^2} + 2\zeta\omega_0\frac{dx}{dt} + \omega_0^2 x = 0, \tag{4}$$

where $\omega_0 = \sqrt{\frac{k}{m}}$ is the (undamped) system's characteristic frequency and $\zeta = \frac{c}{2\sqrt{mk}}$ is the damping ratio. In this work, we consider a specific example from the simple pendulum with the following formulation,

$$\frac{d^2\theta}{dt^2} + \frac{b}{m}\frac{d\theta}{dt} + \frac{g}{L}\sin\theta = 0 \tag{5}$$

in which we set the system with the parameters gravitational constant $g = 9.81$, damping factor $b = 0.15$, pendulum length $l = 1$ and mass $m = 1$. The initial condition at $t = 0$ is with angular displacement $\theta = 0$ and the angular velocity $\dot{\theta} = 3$ rad/sec. We present the QLSTM learning result of the angular velocity $\dot{\theta}$.

The simulation results are shown in Figure 5. Like the previous (sine) case, QLSTM surprisingly learns more on the damped oscillation as early as Epoch 1, refines faster than the classical LSTM (cf. Epoch 15), and has stabler decreasing in loss. We further note two observations: first, the testing loss values are significantly lower than the training ones. The reason is that the testing set (on the right of the red dashed line) has smaller amplitude compared to the training set. After the training, both the training and testing loss converge to a low value. Second, while both QLSTM and LSTM have undershots at the local minima/maxima (cf. Epoch 100), QLSTM's symptom is milder. In addition, QLSTM does not have overshots as seen in the LSTM (Epoch 30).

With these two case studies, we hope to establish that the QLSTM's advantages we see are a common pattern that is portable across different input functions, as we will see below.
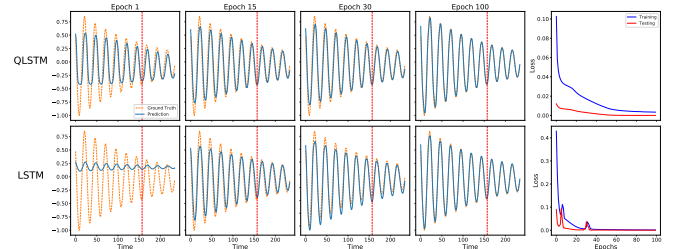
Fig. 5: Learning damped oscillations. The QLSTM learns faster and predicts more accurately than the classical LSTM with a fixed number of epochs. The orange dashed line represents the ground truth $\dot{\theta}$ [that we train the (Q)LSTM to learn] while the blue solid line is the output from the (Q)LSTM. The vertical red dashed line separates the *training* set (left) from the *testing* set (right).

	Training Loss	Testing Loss
QLSTM	2.92×10^{-2}	6×10^{-3}
LSTM	3.15×10^{-2}	5×10^{-3}

Table 2: The comparison of loss values at Epoch 15 for the damped oscillator experiment.

4.2.2. Bessel functions

Bessel functions of the first kind, $J_\alpha(x)$, obeys the following differential equation

$$x^2 \frac{d^2 y}{dx^2} + x \frac{dy}{dx} + \left(x^2 - \alpha^2\right) y = 0, \qquad (6)$$

to which the solution is

$$J_\alpha(x) = \sum_{m=0}^{\infty} \frac{(-1)^m}{m! \Gamma(m + \alpha + 1)} \left(\frac{x}{2}\right)^{2m+\alpha}, \qquad (7)$$

where $\Gamma(x)$ is the Gamma function. Bessel functions are also commonly encountered in physics and engineering problems, such as electromagnetic fields or heat conduction in a cylindrical geometry.

In this example, we choose J_2 for the training. The results are shown in Figure 6. As in the case of damped oscillation, QLSTM learns faster, converges stabler, and has a milder symptom in undershooting. It is particularly interesting to note the poor prediction made by the LSTM at Epoch 1 and 15, in sharp contrast to that by the QLSTM.
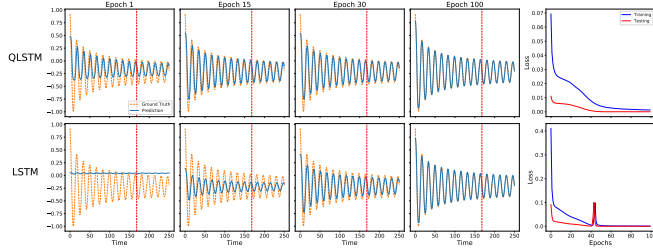
Fig. 6: Learning the Bessel function of order 2 (J_2). QLSTM's performance in prediction and convergence is even better than LSTM's with a slightly more complicated input (a non-exponential decay) compared to the previous cases. The orange dashed line represents the ground truth J_2 [that we train the (Q)LSTM to learn] while the blue solid line is the output from the (Q)LSTM. The vertical red dashed line separates the *training* set (left) from the *testing* set (right).

	Training Loss	Testing Loss
QLSTM	2.26×10^{-2}	5.5×10^{-3}
LSTM	5.43×10^{-2}	1.28×10^{-2}

Table 3: The comparison of loss values at Epoch 15 for the Bessel function J_2 experiment.

4.3. Quantum Control Application

We consider a system with delayed quantum feedback: a two-level atom (or qubit) coupled to a semi-infinite, one-dimensional waveg-

uide, one end of which is terminated by a perfect mirror that 100% reflects any incoming propagating photons. This system can be cast to an open quantum system (OQS) problem by treating the waveguide as the environment seen by the qubit, and in this context it is known to be non-Markovian [37, 38, 39], in particular when the qubit-mirror separation, denoted by L, is an integer multiple of the qubit's resonant wavelength λ_0. Due to the delayed feedback (photons taking round trips to bounce in-between the qubit and the mirror) a bound state in the continuum (BIC) is formed in this case, causing a portion of incoming photons trapped in the interspace between the qubit and the mirror [40, 37, 41]. By "shaking", or modulating, the qubit frequency in time so as to change λ_0 and break the resonant condition, the trapped photon can be released to the waveguide and detected by measuring the output field intensity [37]. In Figure 7 we learn this temporal dependence using (Q)LSTM.
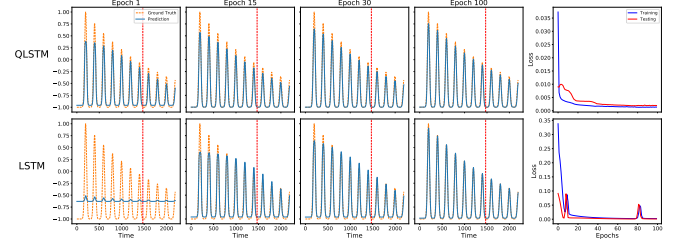
Fig. 7: Learning the dynamics with delayed quantum feedback. The QLSTM fits the local minima better than the LSTM does. The orange dashed line represents the ground truth while the blue solid line is the output from the (Q)LSTM. The vertical red dashed line separates the *training* set (left) from the *testing* set (right).

In this example, we consider a sinusoidal modulation of the qubit frequency such that the average frequency satisfies the resonant condition [37], and the result is shown in Figure 7. Not only are QLSTM's advantages carried over to this case, but it also predicts better at the local minima than the LSTM does (cf. Epoch 100). In particular, note that QLSTM's training loss is almost one order of magnitude smaller than LSTM's by Epoch 15 (see Table 4).

	Training Loss	Testing Loss
QLSTM	2.88×10^{-3}	5.7×10^{-3}
LSTM	1.44×10^{-2}	4.7×10^{-3}

Table 4: The comparison of loss values at Epoch 15 for the delayed quantum control experiment.

5. CONCLUSION AND OUTLOOK

We provide and study the first hybrid quantum-classical model of long short-term memory (QLSTM) which is able to learn data with temporal dependency. We show that under the constraint of similar number of parameters, the QLSTM learns significantly more information than the LSTM does right after the first training epoch, and its loss decreases more stably and faster than that of its classical counterpart. It also learns the local features (minima, maxima, etc) better than the LSTM does in general, especially when the input data has a complicated temporal structure. Our work paves the way toward using quantum circuits to model sequential data or physical dynamics, and strengthens the potential applicability of QML to many other scientific problems or commercial applications.

6. REFERENCES

[1] Karen Simonyan and Andrew Zisserman, "Very deep convolutional networks for large-scale image recognition," in *International Conference on Learning Representations*, 2015.

[2] Christian Szegedy, Wei Liu, Yangqing Jia, Pierre Sermanet, Scott Reed, Dragomir Anguelov, Dumitru Erhan, Vincent Vanhoucke, and Andrew Rabinovich, "Going deeper with convolutions," in *Proceedings of the IEEE conference on computer vision and pattern recognition*, 2015, pp. 1–9.

[3] Athanasios Voulodimos, Nikolaos Doulamis, Anastasios Doulamis, and Eftychios Protopapadakis, "Deep Learning for Computer Vision: A Brief Review," *Computational Intelligence and Neuroscience*, vol. 2018, pp. 1–13, 2018.

[4] Ilya Sutskever, Oriol Vinyals, and Quoc V Le, "Sequence to sequence learning with neural networks," in *Advances in neural information processing systems*, 2014, pp. 3104–3112.

[5] David Silver, Aja Huang, Chris J. Maddison, Arthur Guez, Laurent Sifre, George van den Driessche, Julian Schrittwieser, Ioannis Antonoglou, Veda Panneershelvam, Marc Lanctot, Sander Dieleman, Dominik Grewe, John Nham, Nal Kalchbrenner, Ilya Sutskever, Timothy Lillicrap, Madeleine Leach, Koray Kavukcuoglu, Thore Graepel, and Demis Hassabis, "Mastering the game of Go with deep neural networks and tree search," *Nature*, vol. 529, no. 7587, pp. 484–489, 1 2016.

[6] Alex Graves, Navdeep Jaitly, and Abdel-rahman Mohamed, "Hybrid speech recognition with deep bidirectional lstm," in *2013 IEEE workshop on automatic speech recognition and understanding*. IEEE, 2013, pp. 273–278.

[7] Emmanuel Flurin, Leigh S Martin, Shay Hacohen-Gourgy, and Irfan Siddiqi, "Using a recurrent neural network to reconstruct quantum dynamics of a superconducting qubit from physical observations," *Physical Review X*, vol. 10, no. 1, pp. 011006, 2020.

[8] Moritz August and Xiaotong Ni, "Using recurrent neural networks to optimize dynamical decoupling for quantum memory," *Physical Review A*, vol. 95, no. 1, pp. 012335, 2017.

[9] Andrew Cross, "The ibm q experience and qiskit open-source quantum computing software," in *APS Meeting Abstracts*, 2018.

[10] Frank Arute, Kunal Arya, Ryan Babbush, Dave Bacon, Joseph C Bardin, Rami Barends, Rupak Biswas, Sergio Boixo, Fernando GSL Brandao, David A Buell, et al., "Quantum supremacy using a programmable superconducting processor," *Nature*, vol. 574, no. 7779, pp. 505–510, 2019.

[11] Trevor Lanting, Anthony J Przybysz, A Yu Smirnov, Federico M Spedalieri, Mohammad H Amin, Andrew J Berkley, Richard Harris, Fabio Altomare, Sergio Boixo, Paul Bunyk, et al., "Entanglement in a quantum annealing processor," *Physical Review X*, vol. 4, no. 2, pp. 021041, 2014.

[12] John Preskill, "Quantum computing in the nisq era and beyond," *Quantum*, vol. 2, pp. 79, 2018.

[13] Daniel Gottesman, "Stabilizer codes and quantum error correction," *arXiv preprint quant-ph/9705052*, 1997.

[14] Daniel Gottesman, "Theory of fault-tolerant quantum computation," *Physical Review A*, vol. 57, no. 1, pp. 127, 1998.

[15] Kosuke Mitarai, Makoto Negoro, Masahiro Kitagawa, and Keisuke Fujii, "Quantum circuit learning," *Physical Review A*, vol. 98, no. 3, pp. 032309, 2018.

[16] Yuxuan Du, Min-Hsiu Hsieh, Tongliang Liu, and Dacheng Tao, "The expressive power of parameterized quantum circuits," *arXiv preprint arXiv:1810.11922*, 2018.

[17] Maria Schuld, Alex Bocharov, Krysta Svore, and Nathan Wiebe, "Circuit-centric quantum classifiers," *arXiv preprint arXiv:1804.00633*, 2018.

[18] Vojtěch Havlíček, Antonio D Córcoles, Kristan Temme, Aram W Harrow, Abhinav Kandala, Jerry M Chow, and Jay M Gambetta, "Supervised learning with quantum-enhanced feature spaces," *Nature*, vol. 567, no. 7747, pp. 209–212, 2019.

[19] Pierre-Luc Dallaire-Demers and Nathan Killoran, "Quantum generative adversarial networks," *Physical Review A*, vol. 98, no. 1, pp. 012324, 2018.

[20] Samuel Yen-Chi Chen, Chao-Han Huck Yang, Jun Qi, Pin-Yu Chen, Xiaoli Ma, and Hsi-Sheng Goan, "Variational quantum circuits for deep reinforcement learning," *IEEE Access*, vol. 8, pp. 141007–141024, 2020.

[21] Maria Schuld and Francesco Petruccione, *Supervised learning with quantum computers*, vol. 17, Springer, 2018.

[22] Jacob Biamonte, Peter Wittek, Nicola Pancotti, Patrick Rebentrost, Nathan Wiebe, and Seth Lloyd, "Quantum machine learning," *Nature*, vol. 549, no. 7671, pp. 195–202, 2017.

[23] Vedran Dunjko and Hans J Briegel, "Machine learning & artificial intelligence in the quantum domain: a review of recent progress," *Reports on Progress in Physics*, vol. 81, no. 7, pp. 074001, 2018.

[24] Abhinav Kandala, Antonio Mezzacapo, Kristan Temme, Maika Takita, Markus Brink, Jerry M Chow, and Jay M Gambetta, "Hardware-efficient variational quantum eigensolver for small molecules and quantum magnets," *Nature*, vol. 549, no. 7671, pp. 242–246, 2017.

[25] Edward Farhi, Jeffrey Goldstone, and Sam Gutmann, "A quantum approximate optimization algorithm," *arXiv preprint arXiv:1411.4028*, 2014.

[26] Jarrod R McClean, Jonathan Romero, Ryan Babbush, and Alán Aspuru-Guzik, "The theory of variational hybrid quantum-classical algorithms," *New Journal of Physics*, vol. 18, no. 2, pp. 023023, 2016.

[27] Edward Farhi and Hartmut Neven, "Classification with quantum neural networks on near term processors," *arXiv preprint arXiv:1802.06002*, 2018.

[28] Marcello Benedetti, Erika Lloyd, Stefan Sack, and Mattia Fiorentini, "Parameterized quantum circuits as machine learning models," *Quantum Science and Technology*, vol. 4, no. 4, pp. 043001, 2019.

[29] Andrea Mari, Thomas R Bromley, Josh Izaac, Maria Schuld, and Nathan Killoran, "Transfer learning in hybrid classical-quantum neural networks," *arXiv preprint arXiv:1912.08278*, 2019.

[30] Sukin Sim, Peter D Johnson, and Alán Aspuru-Guzik, "Expressibility and entangling capability of parameterized quantum circuits for hybrid quantum-classical algorithms," *Advanced Quantum Technologies*, vol. 2, no. 12, pp. 1900070, 2019.

[31] Kurt Hornik, Maxwell Stinchcombe, Halbert White, et al., "Multilayer feedforward networks are universal approximators.," *Neural networks*, vol. 2, no. 5, pp. 359–366, 1989.

[32] Adam Paszke, Sam Gross, Francisco Massa, Adam Lerer, James Bradbury, Gregory Chanan, Trevor Killeen, Zeming Lin, Natalia Gimelshein, Luca Antiga, Alban Desmaison, Andreas Kopf, Edward Yang, Zachary DeVito, Martin Raison, Alykhan Tejani, Sasank Chilamkurthy, Benoit Steiner, Lu Fang, Junjie Bai, and Soumith Chintala, "PyTorch: An Imperative Style, High-Performance Deep Learning Library," in *Advances in Neural Information Processing Systems 32*, H. Wallach and H. Larochelle and A. Beygelzimer and F. d'Alché-Buc and E. Fox and R. Garnett, Ed., pp. 8024–8035. Curran Associates, Inc., 2019.

[33] Ville Bergholm, Josh Izaac, Maria Schuld, Christian Gogolin, Carsten Blank, Keri McKiernan, and Nathan Killoran, "Pennylane: Automatic differentiation of hybrid quantum-classical computations," *arXiv preprint arXiv:1811.04968*, 2018.

[34] "Pennylane-Qulacs plugin," https://github.com/PennyLaneAI/pennylane-qulacs, Originally written by Steven Oud (@soudy).

[35] "Qulacs," https://github.com/qulacs/qulacs, 2018.

[36] T. Tieleman and G. Hinton, "Lecture 6.5—RmsProp: Divide the gradient by a running average of its recent magnitude," COURSERA: Neural Networks for Machine Learning, 2012.

[37] Tommaso Tufarelli, Francesco Ciccarello, and M. S. Kim, "Dynamics of spontaneous emission in a single-end photonic waveguide," *Phys. Rev. A*, vol. 87, pp. 013820, Jan 2013.

[38] T. Tufarelli, M. S. Kim, and F. Ciccarello, "Non-Markovianity of a quantum emitter in front of a mirror," *Phys. Rev. A*, vol. 90, no. 1, pp. 012113, July 2014.

[39] Yao-Lung L Fang, Francesco Ciccarello, and Harold U Baranger, "Non-Markovian dynamics of a qubit due to single-photon scattering in a waveguide," *New J. Phys.*, vol. 20, no. 4, pp. 043035, Apr. 2018.

[40] H. Dong, Z.R. Gong, H. Ian, Lan Zhou, and C.P. Sun, "Intrinsic cavity QED and emergent quasinormal modes for a single photon," *Phys. Rev. A*, vol. 79, pp. 063847, Jun 2009.

[41] Giuseppe Calajo, Yao-Lung L Fang, Harold U Baranger, and Francesco Ciccarello, "Exciting a Bound State in the Continuum through Multiphoton Scattering Plus Delayed Quantum Feedback," *Phys. Rev. Lett.*, vol. 122, no. 7, pp. 073601, Feb. 2019.